

Analysis of Nose Cone of Missile

P. KIRAN KUMAR

Assistant Professor, Department of Mechanical Engineering,
CBIT, Hyderabad, India

ABSTRACT

Nose cone is the forward most section of a rocket, guided missile or aircraft. In guided missile nose cone although reduces the drag force, should also serve the purpose of storing and protecting payload (warhead, guiding systems) until the target is reached. In this work an attempt is made to compare two different nose cone profiles with near same payload capacity. The effect of pressure, velocity and various other parameters are analyzed using ANSYS FLUENT software. The analysis will be carried out for two models of nose cone namely Conical and Tangent Ogive nose cone for supersonic flow of different Mach numbers.

KEY WORDS: Nose cone, lift, drag, Mach number

Date of Submission: 20-06-2020

Date of Acceptance: 07-07-2020

I. INTRODUCTION

1.1.1 LIFT

A fluid flowing over the surface of a body exerts a force on it. It makes no difference whether the fluid is flowing past a stationary body or the body is moving through a stationary volume of fluid. Lift is the component of this force that is perpendicular to the oncoming flow direction. Lift is always accompanied by a drag force, which is the component of the surface force parallel to the flow direction. Lift is most commonly associated with the wings of fixed-wing aircraft, although it is more generally generated by many other streamlined bodies such as propellers, kites, helicopter rotors, racing car wings, maritime sails, and wind turbines in air, and by sailboat keels, ship's rudders, and hydrofoils in water.

1.1.2 LIFT COEFFICIENT

The lift coefficient (C_L , C_N or C_Z) is a dimensionless coefficient that relates the lift generated by a lifting body to the fluid density around the body, the fluid velocity and an associated reference area. The lift coefficient C_L is defined by:

$$C_L \equiv \frac{L}{q S} = \frac{L}{\frac{1}{2} \rho u^2 S} = \frac{2L}{\rho u^2 S}$$

where L is the lift force, S is the relevant surface area and q is the fluid dynamic pressure, in turn

linked to the fluid density ρ , and to the flow

speed u . The choice of the reference surface should be specified since it is arbitrary

1.1.3 DRAG

In fluid dynamics, drag (sometimes called air resistance, a type of friction, or fluid resistance, another type of friction or fluid friction) is a force acting opposite to the relative motion of any object moving with respect to a surrounding fluid. This can exist between two fluid layers (or surfaces) or a fluid and a solid surface. Unlike other resistive forces, such as dry friction, which are nearly independent of velocity, drag forces depend on velocity. Drag force is proportional to the velocity for a laminar flow and the squared velocity for a turbulent flow. Even though the ultimate cause of a drag is viscous friction, the turbulent drag is independent of viscosity. Drag forces always decrease fluid velocity relative to the solid object in the fluid's path.

1.1.4 DRAG COEFFICIENT

In fluid dynamics, the drag coefficient (commonly denoted as: C_D , C_X or C_W) is a dimensionless quantity that is used to quantify the drag or resistance of an object in a fluid environment, such as air or water. It is used in the drag equation in which a lower drag coefficient indicates the object will have less aerodynamic or hydrodynamic drag. The drag coefficient is always associated with a particular surface area. The drag coefficient C_D is defined as:

$$c_d = \frac{2F_d}{\rho u^2 A}$$

where: F_D is the drag force, which is by definition the force component in the direction of the flow

velocity ρ is the mass density of the fluid, u is the flow speed of the object relative to the fluid, A is the reference area.

1.2 SUPERSONIC FLOW

In aeronautics, supersonic refers to the condition of flight in which a range of velocities of airflow exist surrounding and flowing past an air vehicle or an airfoil that are concurrently above the speed of sound i.e., Mach number, M , is more than unity.

In other words, fluid motion in which the Mach number M , defined as the speed of the fluid relative to the sonic speed in the same medium, is more than unity is known as supersonic flow. It is, however, common to call the flow transonic when $0.8 < M < 1.4$, and hypersonic when $M > 5$.

1.3 MACH WAVES

A particle moving in a compressible medium, such as air, emits acoustic disturbances in the form of spherical waves. These waves propagate at the speed of sound ($M=1$). If the particle moves at a supersonic speed, the generated waves cannot propagate upstream of the particle. The spherical waves are enveloped in a circular cone called the Mach cone. The generators of the Mach cone are called Mach lines or Mach waves.

1.4 SHOCK WAVES

When a fluid at a supersonic speed approaches an airfoil (or a high-pressure region), no information is communicated ahead of the airfoil, and the flow adjusts to the downstream conditions through a shock wave. Shock waves propagate faster than Mach waves and the low speed changes abruptly from supersonic to less than supersonic or subsonic across the wave. Similarly, other properties change discontinuously across the wave. A Mach wave is a shock wave of minimum strength. Upstream of a shock wave is always supersonic.

1.5 NOSE CONE

The term Nose Cone is used to refer to the forward most section of an aircraft, rocket, guided missile and Aerial vehicle. The cone is shaped to offer minimum aerodynamic resistance. Nose cones are also designed for travel in and under water and in high-speed land vehicles. Due to the extreme temperatures involved, nose cones for high-speed applications have to be made of refractory materials. Pyrolytic carbon is one choice,

reinforced carbon-carbon composite or HRSI ceramics are other popular choices.

1.6 TYPES OF NOSE CONES

Given the problem of the aerodynamic design of the nose cone section of any vehicle or body meant to travel through a compressible fluid medium an important problem is the determination of the nose cone geometrical shape for optimum performance. For many applications, such a task requires the definition of a solid of revolution shape that experiences minimal resistance to rapid motion through such a fluid medium, which consists of elastic particles.

In all of the following nose cone shape equations, L is the overall length of the nose cone and R is the radius of the base of the nose cone. y is the radius at any point x , as x varies from 0, at the tip of the nose cone, to L . The equations define the 2-dimensional profile of the nose shape. The full body of revolution of the nose cone is formed by rotating the profile around the centerline (C/L). While the equations describe the "perfect" shape, practical nose cones are often blunted or truncated for manufacturing or aerodynamic reasons.

1.6.1 CONICAL

A very common nose-cone shape is a simple cone. This conical shape is often chosen for its ease of manufacture, and is also often chosen for its drag and radar crosssection characteristics. A lower drag cone would be more streamlined, with the most optimal shape being a Sears-Haack body. The sides of a conical profile are straight lines, so the diameter equation is simply

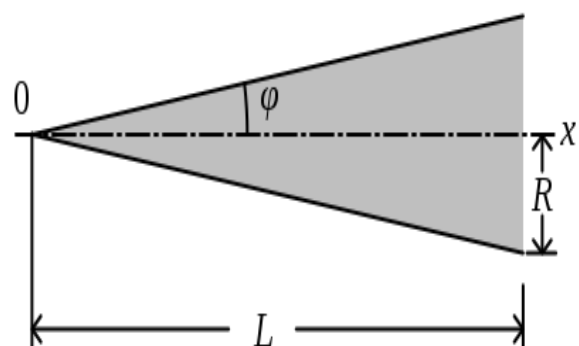


Figure 1.1 Conical Nose Cone

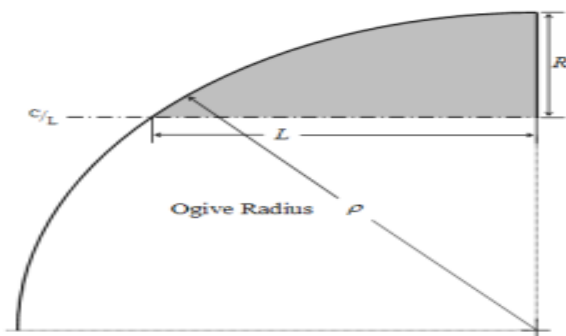


Figure 1.2 Tangent Ogive Nose Cone

1.6.2 TANGENT OGIVE

Next to a simple cone, the tangent ogive shape is the most familiar in hobby rocketry. The profile of this shape is formed by a segment of a circle such that the rocket body is tangent to the curve of the nose cone at its base, and the base is on the radius of the circle. The popularity of this shape is largely due to the ease of constructing its profile. The radius of the circle that forms the ogive is called the ogive radius. The nose cone length, L , must be less than or equal to ogive radius. If they are equal it is called hemisphere

II. PROBLEM STATEMENT

2.1 An aircraft travelling at supersonic speed is subjected to lift and drag forces. These forces vary for different nose cone designs. In this work we try to show the same by analyzing two nose cone profiles, namely, conical and tangent ogive nose cone, by using ANSYS FLUENT software. The lift and drag variations along with the pressure and velocity contours can be visualized during the simulations. Also, to visualize the oblique shock waves formed.

2.2 OBJECTIVE

- To study the lift and drag forces for different models of nose cone and their variation based on the nose cone profile.
- To obtain the velocity and pressure contours across the model at different Mach numbers.
- To study the variation of lift and drag coefficients with varying Mach number.
- To understand the shock waves formed at each nose cone profile at different Mach numbers.

III. LITERATURE REVIEW

- Girish Kumar and Dr. Pravin V Honguntikar studied the effect of pressure, velocity and various other parameters by analysis using ANSYS FLUENT software which is custom made to analyze these parameters. The analysis was carried out for three model of nose cone

namely Sharp, Ogive and Blunt nose cone for transonic flow of Mach number 1.

By comparing C_d and drag force for different nose cones, the ideal nose shape for aerial vehicles that minimizes its drag depends on how fast the aerial vehicle is designed to travel. As a result, the ideal nose for a model aerial vehicle is ogive shape. The drag force is more for sharp and blunt nose cone than the ogive nose cone shape.

The analysis of three types of nose cones showed the variation in the pressure, velocity, Mach number around the nose cone of an aerial vehicle. Each nose cone shape results in a certain amount of aerodynamic heating. If the aerodynamic heating is less than the need for thermal protection systems will be reduced.

- A Sanjay Varma, G Sai Sathyanarayana and J Sandeep delivered their efforts in comparing various nose profiles to know performance over existing conventional nose profiles. Flow phenomenon is observed in numerical simulations for different nose cone profiles and presented critical design aspects and performance characteristics of nose cone. Solution is proposed that von Karman ogive nose profile gave higher critical Mach number and minimum pressure coefficient which is desirable for the subsonic flows.
- Shafeeque A P conducted an external flow analysis on atmospheric re-entering vehicle called Apollo AS-202 developed by NASA. Computational fluid dynamics is used to obtain the flow field that develops around re-entry capsules. The heat flux variation, velocity profile, temperature variation and pressure distribution at various locations of the capsules are presented by specifying the appropriate boundary conditions.
- Bogdan-Alexandru Belega has shown that significant performance gains result for adaptation of the exhaust flow to the ambient pressure, to which it was necessary to collect and study various nose cone shapes and the equations describing them. The types of nose cones with ejector channels were identified and aerodynamic characteristics of different types of nose cones were specified.

The design method consisted of a geometry creation step in which a three-dimensional geometry is generated, a mathematical model presented and a simple flow analysis (FLUENT Simulation from SolidWorks and ANSYS simulation with SPH for fluid-structure interaction), step which predicts the air intake mass

flow rate. Performance characteristics of nose cone are presented.

IV. METHODOLOGY

4.1 MODELING OF NOSE CONES

The modeling of each nose cone profile has been done using Solid Works 2017 software. It is solid modeling CAD software produced by Dassault systems. We have used part design capability of this software for creating the models.

4.1.1 MODELING OF CONICAL NOSE CONE

The model of conical nose cone is formed by revolving a triangle with dimension of height being the required length of the nose cone and the base dimension being the radius of the nose cone. The height and base are drawn parallel and perpendicular respectively to the axis of revolution. The side of the triangle which represents height lies on the axis of revolution and the base perpendicular to the same.

Length of conical nose cone : 1975 mm
Diameter of conical nose cone : 760 mm
Cone angle of nose cone : 21.78 degrees



Figure 4.1 Model of Conical Nose Cone

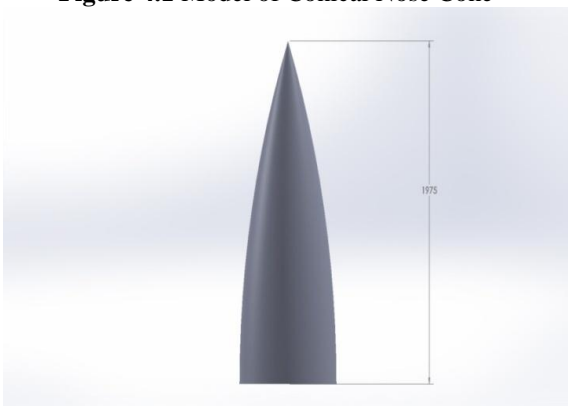


Figure 4.2 Model of Tangent Ogive Nose Cone

4.1.2 MODELING OF TANGENT OGIVE NOSE CONE

In tangent ogive, the center of rotation of the arc is in the plane of the base of the nose cone. Three points are plotted on a plane through which the circle which forms tangent ogive shape, are plotted. A circumference circle is drawn through the three points. The height and base lines are drawn. Similar to the conical shape the height side coincides with the axis of rotation and the base is perpendicular to the same. The unnecessary parts are trimmed off and the shape is revolved about the axis, thus forming the model of tangent ogive cone.
Length of tangent ogive nose cone : 1975 mm
Diameter of tangent ogive nose cone : 760 mm

4.2 ANALYSIS OF NOSE CONES

ANSYS Workbench is an engineering software suite, equipped with many different solvers and project management utilities. It is the main toolbox for this project, used to organize the modeling, meshing, solving and post-processing the parts of different optimizations and simulations. ANSYS FLUENT is used as solver for analysis purpose. Create a new Fluent fluid flow analysis system by double-clicking the Fluid Flow (Fluent) option under Analysis Systems in the Toolbox.

4.2.1 GEOMETRY

For the geometry of the fluid flow analysis, the pre-existing geometry that was created using SOLID WORKS was imported by right-clicking the Geometry cell and selecting the 'Import Geometry' option from the context menu. The geometry was then enclosed in an enclosure of required dimensions, to simulate the flow conditions.

4.2.2 MESH

ANSYS FLUENT uses unstructured meshes in order to reduce the amount of time spent in generating meshes, to simplify the geometry modelling and mesh generation process, to allow modelling of more complex geometries than you can handle with conventional, multi-block structured meshes, and adapts the mesh to resolve the flow-field features. ANSYS FLUENT can also use body-fitted, block-structured meshes. ANSYS FLUENT is capable of handling triangular and quadrilateral elements (or a combination of the two) in 2D, and tetrahedral, hexahedral, pyramid, wedge, and polyhedral elements (or a combination of these) in 3D. This flexibility allows you to pick mesh topologies that are best suited for your particular application, as described in the User's Guide.

The geometry of fluid flow analysis, can be created in ANSYS Design Modeler, or the appropriate geometry file can be imported. If the geometry is created in ANSYS Design Modeler, then the list of files generated by ANSYS Workbench are to be reviewed. In this work the models are created using SOLID WORKS and are imported to ANSYS FLUENT by storing the files in step format.

After importing the geometry a computational mesh is generated throughout the flow volume. In order to simplify the work later on in ANSYS FLUENT, each boundary in the geometry is labelled by creating named selections for the inlet, the outlet, and the cone surface. The outer wall boundaries are automatically detected by ANSYS FLUENT.

Using the 'Generate Mesh' option the mesh was created. By using the 'Update' option the mesh was generated automatically, the relevant mesh files for the project are created, and the ANSYS Workbench cell that references this mesh is updated.

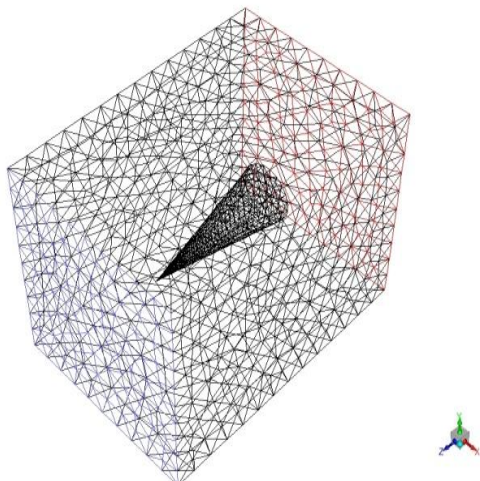


Figure 4.3 Mesh of Enclosure for Conical Nose Cone

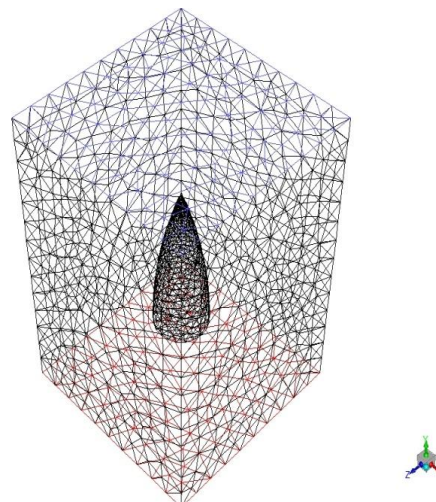


Figure 4.4 Mesh of Enclosure for Tangent Ogive Nose Cone

4.2.3 SETUP

After creating a computational mesh for the geometry, in this step a CFD analysis using ANSYS FLUENT is set up.

In the ANSYS Workbench, double-click the 'Setup cell' in the fluid flow analysis system or also right-click the Setupcell to display the context menu where the 'Edit' option is selected. When ANSYS Fluent is first started, the Fluent Launcher is displayed.

The required changes are made in the 'general' and the 'models' sections of the setup tree as per the type of analysis being conducted. The fluid is selected and its properties are assigned as per the flow conditions. The selection of nose cone material is not required. The cell zone conditions are verified and the boundary conditions are given, which are the flow velocity and gauge pressure. The reference values are updated.

In the 'Monitors' section under solution, the parameters to be plotted are added, which are coefficient of drag, C_D and coefficient of lift, C_L .

The solution is initialized after all the parameters required are being accorded. Then the calculations are made by selecting 'run calculation' from the set up tree. The number of iterations required is to be mentioned and then by clicking the calculate icon the calculations are started. The solution will be stopped after the residuals reach the specified value of iterations. The required contours can be generated from the results section of FLUENT.

V. RESULTS

The results are extracted from CFD post after the analysis from FLUENT solver as shown in the below figures. These results give the coefficient of drag, pressure and velocity distribution over the

nose cone shapes and the shock wave formed due to the supersonic flow.

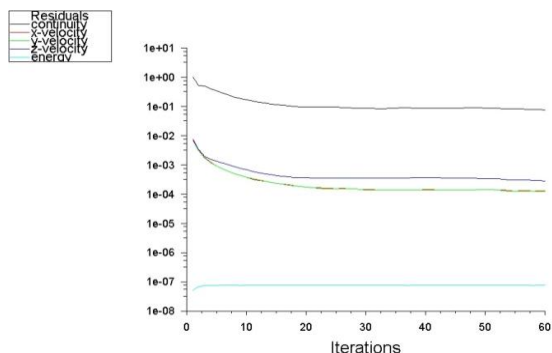


Figure 5.1 Convergence using Residual Values

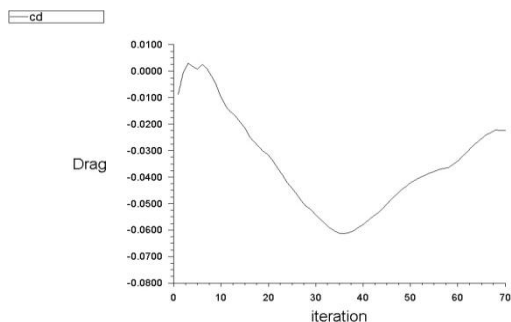


Figure 5.2 C_D for conical nose cone

The above graph represents the coefficient of drag of a conical nose cone subjected to a fluid flow of Mach number 2. The variation of C_D with each iteration can be observed. The negative sign indicates that the drag is in direction opposite to the coordinate axis.

Convergence-criteria is path to followed by solution to eliminate non linearities in solution. From the above figure it can be stated that the analysis holds good as convergence is reached. For each analysis it is taken care that the convergence is attained and from the results it was observed that the convergence attains at near same iteration for all the analyses.

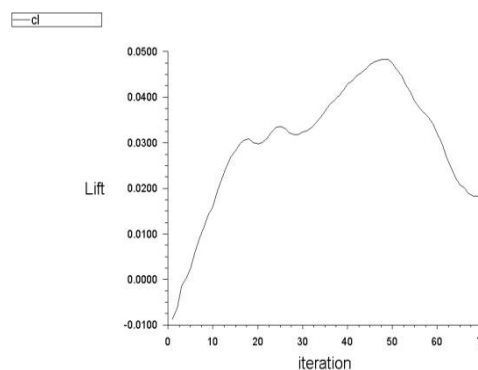


Figure 5.3 C_L for Conical Nose Cone

The above picture gives information regarding the pressure distribution or contour across a conical nose cone in a flow at Mach number 2. The red color at the tip of the nose cone indicates that the pressure is very high at that place.

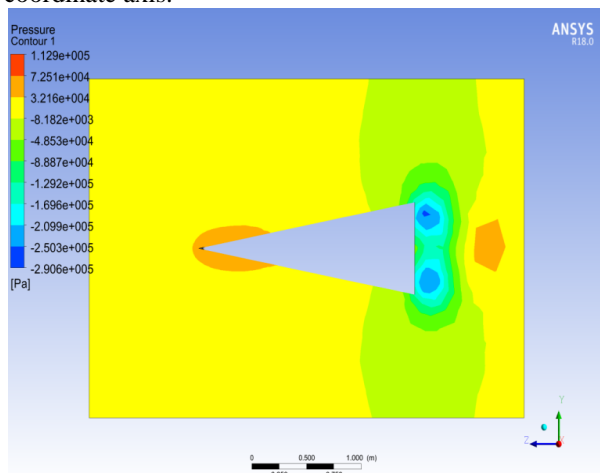


Figure 5.4 Pressure Contour for Conical Nose Cone

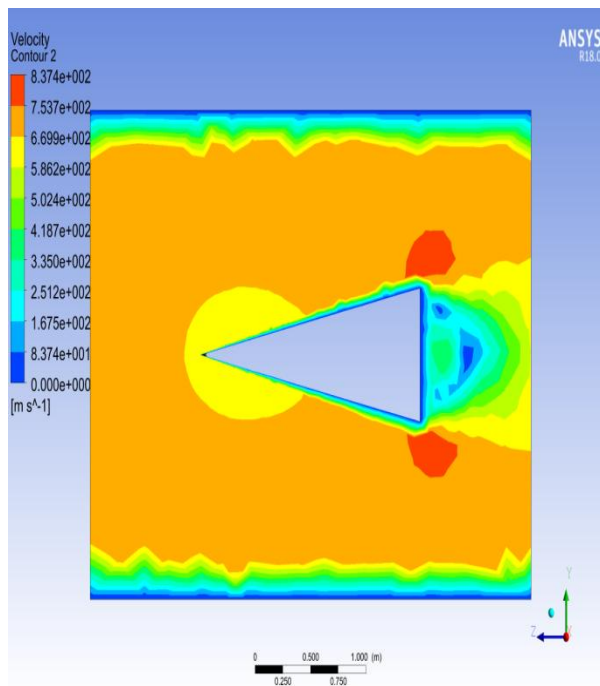


Figure 5.5 Velocity Contour for Conical Nose Cone

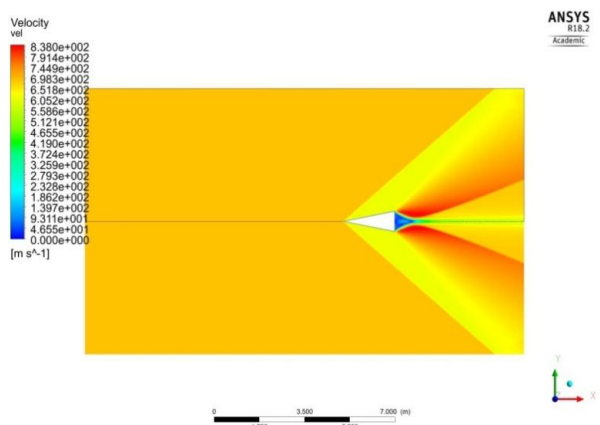


Figure 5.6 Shock Wave for Conical Nose cone

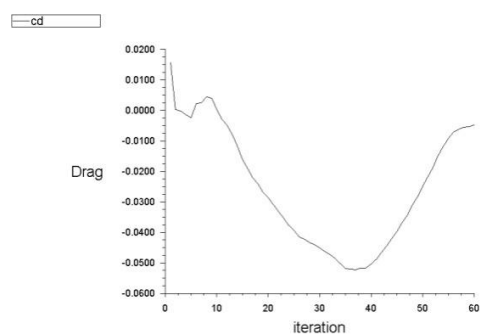


Figure 5.7 C_D for Tangent Ogive Nose Cone

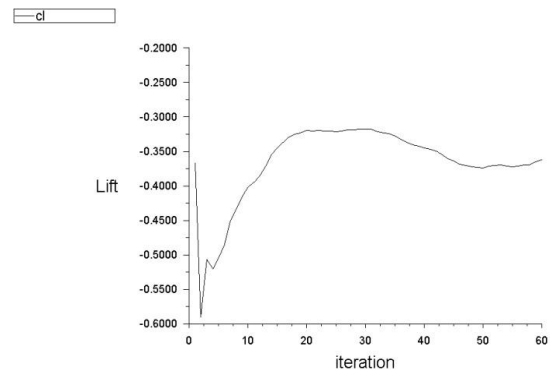


Figure 5.8 C_L for Tangent Ogive Nose Cone

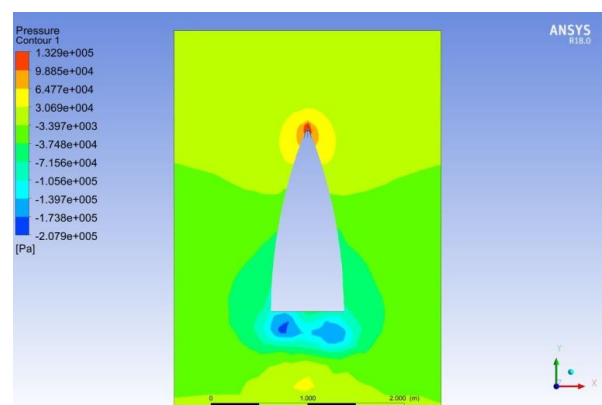


Figure 5.9 Pressure Contour for Tangent Ogive Nose Cone

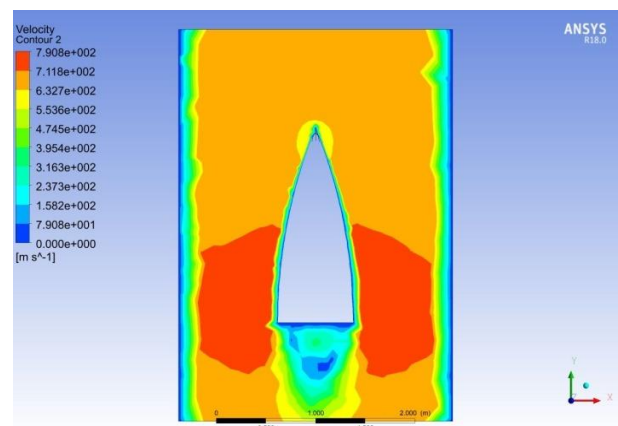


Figure 5.10 Velocity Contour for Tangent Ogive Nose Cone

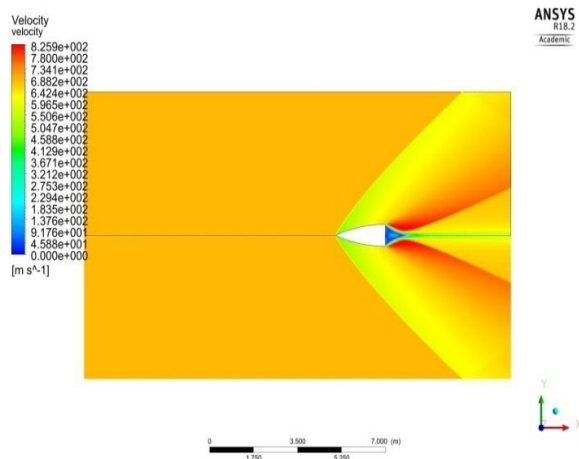


Figure 5.61 Shock Wave for Tangent Ogive Nose Cone

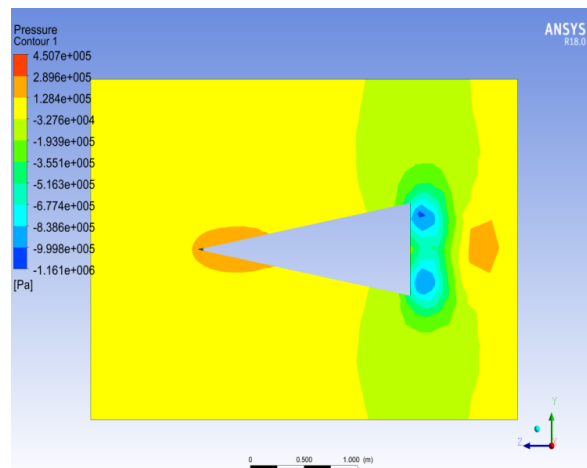


Figure 5.14 Pressure Contour for Conical Nose Cone

5.2 AT MACH NUMBER, $M=3$

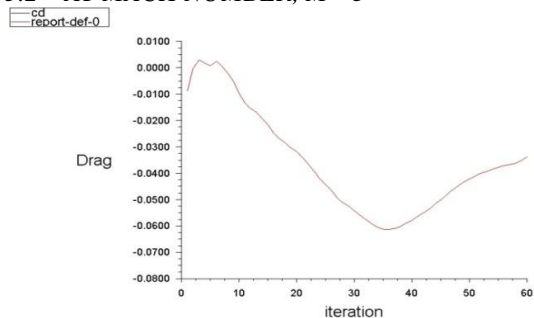


Figure 5.72 C_D for conical nose cone

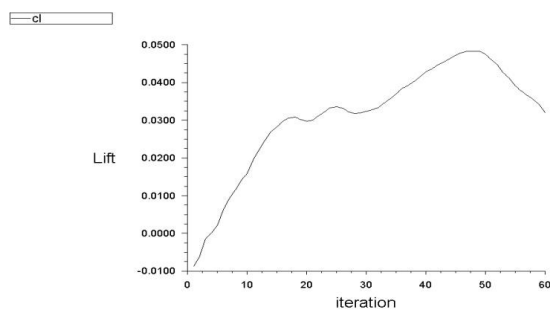


Figure 5.13 C_L for conical nose cone

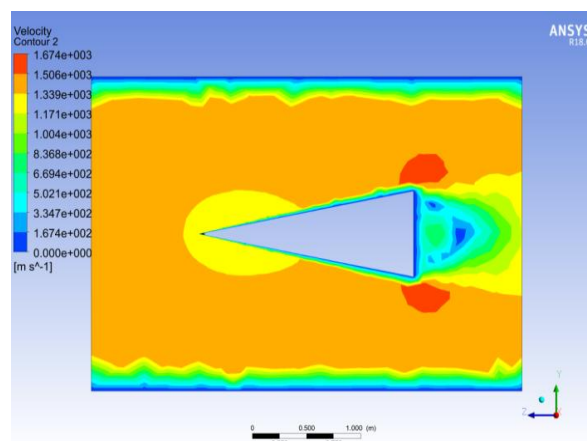


Figure 5.15 Velocity Contour for Conical Nose Cone

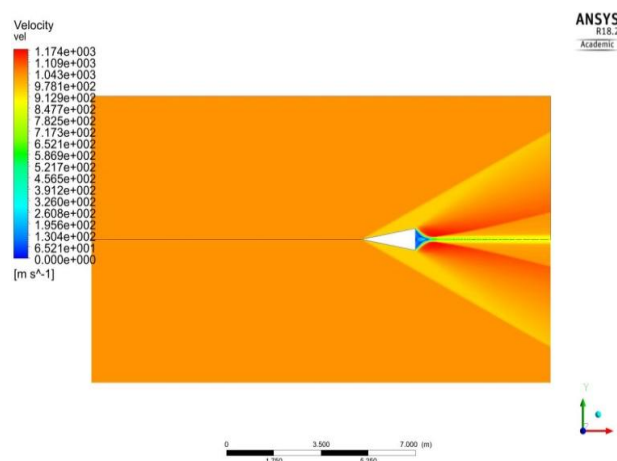


Figure 5.16 Shock Wave for Conical Nose cone

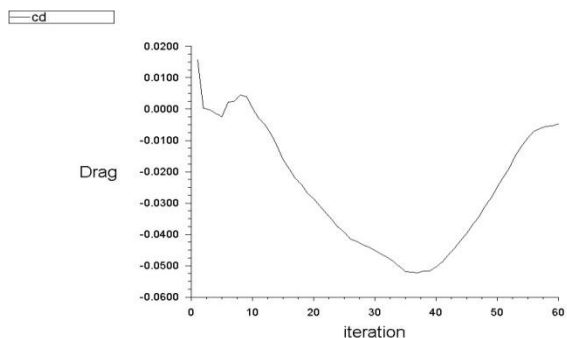


Figure 5.17 C_D for Tangent Ogive Nose Cone

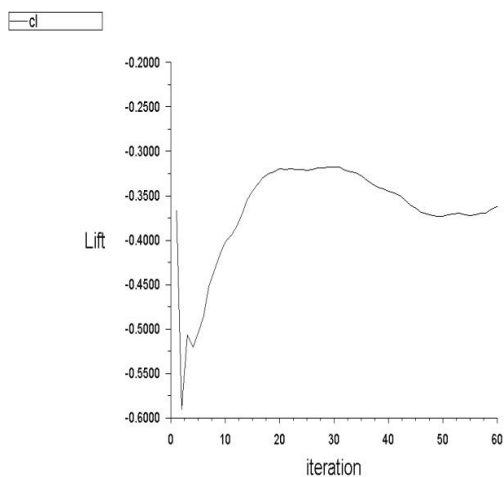


Figure 5.18 C_L for Tangent Ogive Nose Cone

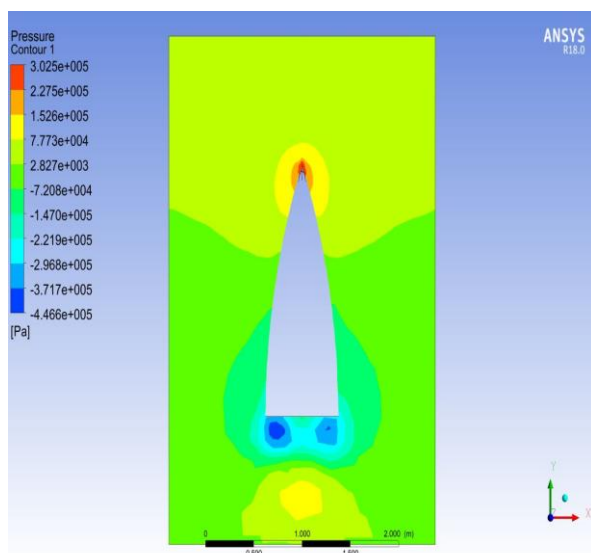


Figure 5.19 Pressure Contour for Tangent Ogive Nose Cone

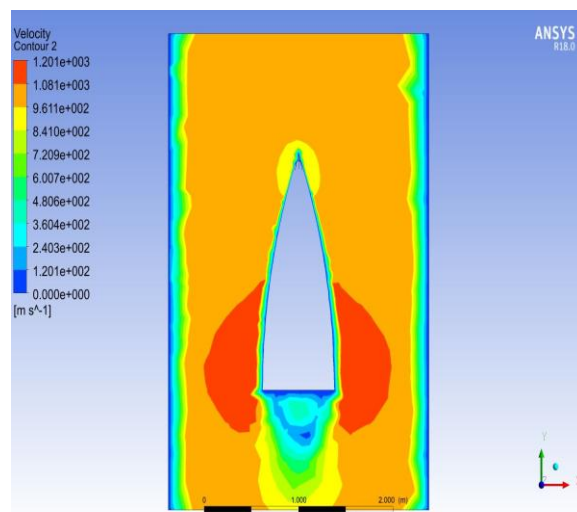


Figure 5.20 Velocity Contour for Tangent Ogive Nose Cone

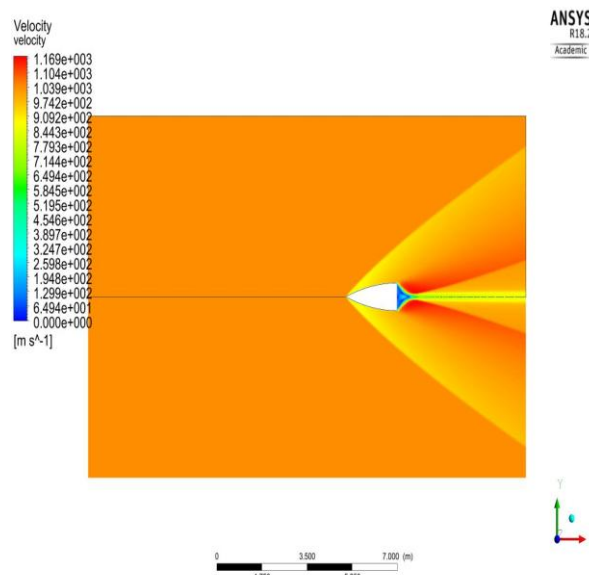


Figure 5.21 Shock Wave for Tangent Ogive Nose Cone

5.3 AT MACH NUMBER, $M=4$

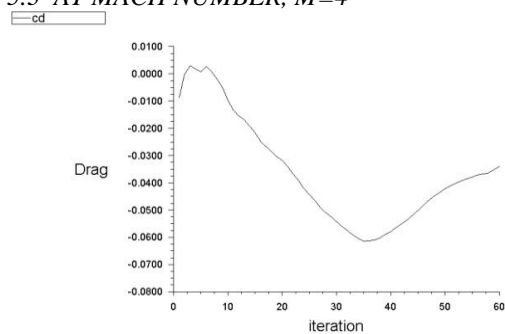


Figure 5.22 C_D for conical nose cone

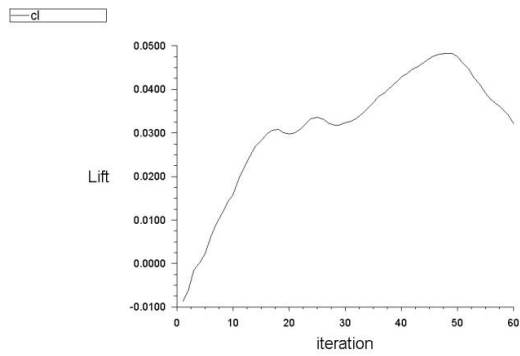


Figure 5.23 C_L for conical nose cone

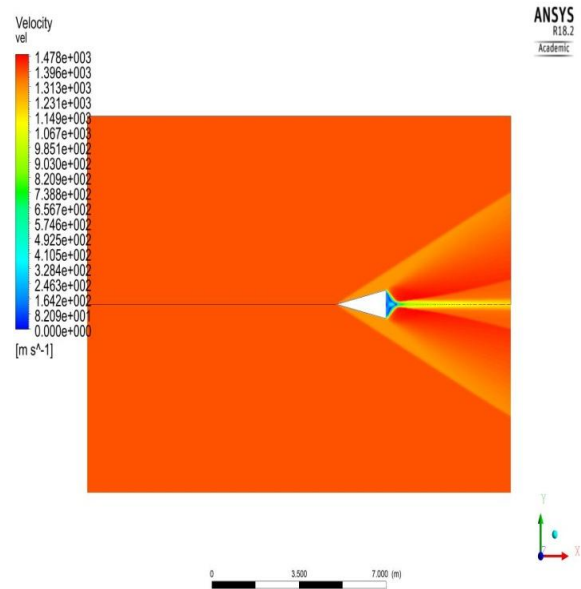


Figure 5.26 Shock Wave for Conical Nose cone

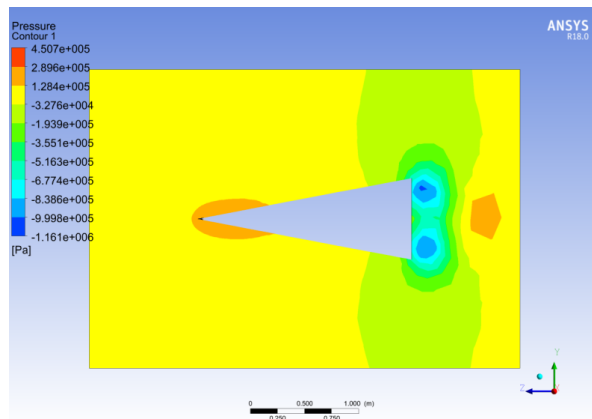


Figure 5.24 Pressure Contour for Conical Nose Cone

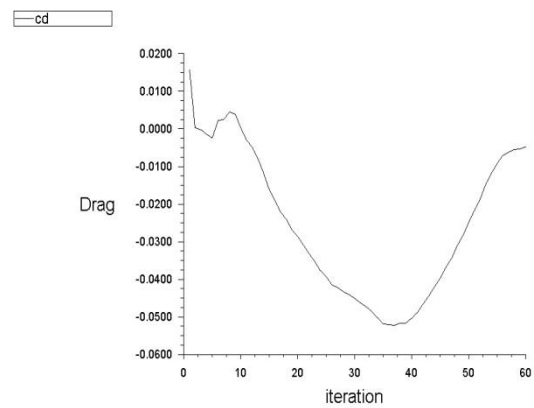


Figure 5.279 C_D for Tangent Ogive Nose Cone

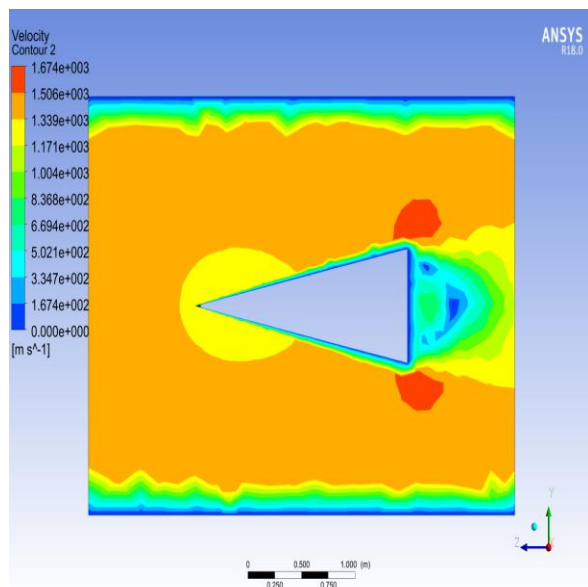


Figure 5.25 Velocity Contour for Conical Nose Cone

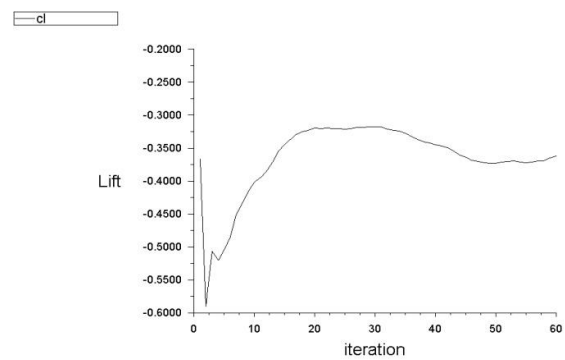


Figure 5.28 C_L for Tangent Ogive Nose Cone

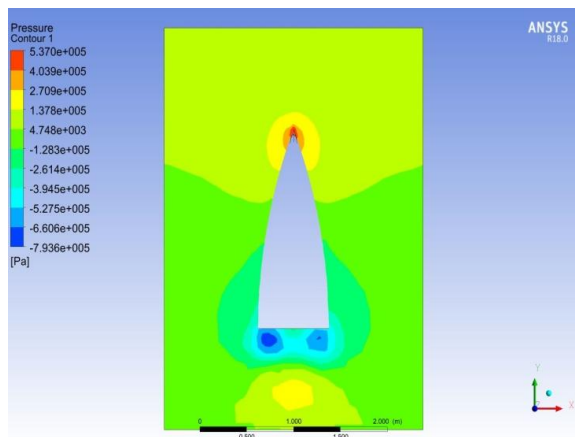


Figure 5.29 Pressure Contour for Tangent Ogive Nose Cone

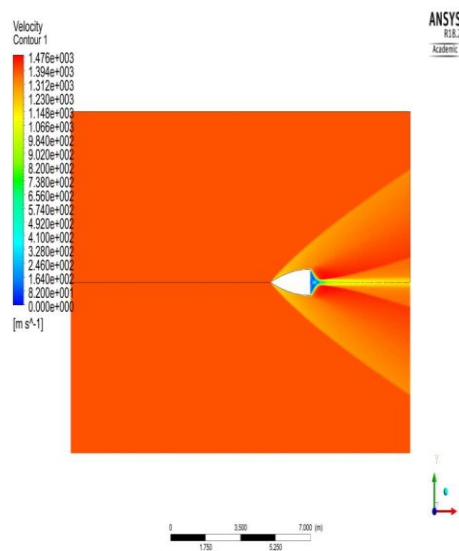


Figure 5.11 Shock Wave for Tangent Ogive Nose Cone

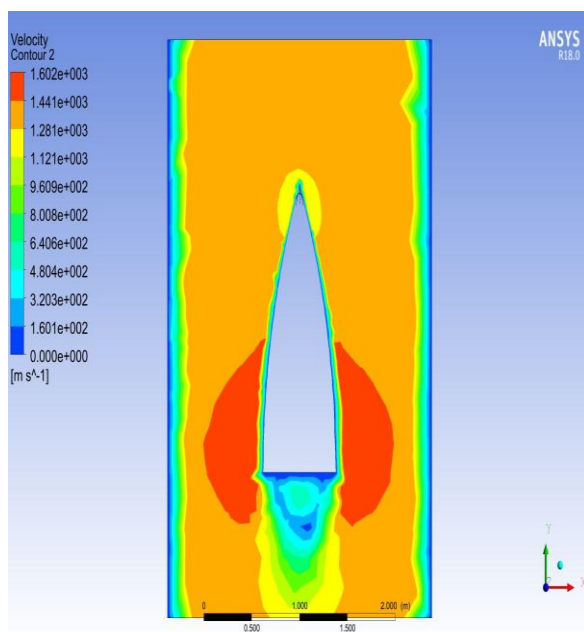


Figure 5.100 Velocity Contour for Tangent Ogive Nose Cone

VI. CONCLUSION

From the above results it can be stated that drag coefficient of tangent ogive nose cone is less compared to conical nose cone, so drag force is less for tangent ogive nose cone. As aerodynamic heating is directly proportional to drag force on surface of nose cone tangent ogive nose cone can be considered for less aerodynamic heating design. The Tangent ogive nose cone is easy to manufacture, has good aerodynamic characteristics and experiences the least amount of aerodynamic heating. It also provides flexibility in the selection of material for the nose cone as the aerodynamic heating is less.

From the pressure and velocity contours it has been observed that at all the Mach numbers, in

tangent ogive nose cone, the pressure variation across the apex shows that the reduction in velocity is maximum at that point when compared to other edges of nose cone and this region of high pressure or low velocity is confined to only the apex or tip in case of conical nose cone. The aerodynamic shape of the tangent ogive structure is more gradual when compared to conical nose cone.

As observed in the result of shock waves at different Mach numbers for the same profile it is evident that the oblique shock wave angle decreases with increase in Mach number and for different profiles at same Mach number the oblique shock wave formed at the apex of tangent ogive nose cone is comparatively stronger than that formed at the apex of conical nose cone.

REFERENCES

- [1]. T V Karthikeyan, A K Kapoor, "Guided Missiles", DRDO Metcalfe House, Delhi, 1990.
- [2]. AK Sreekanth, "Aerodynamic predictive methods and their validation in hypersonic flows", DRDO India.
- [3]. B. Tyler Brooker Semih M. Olcmen, John Baker and Keith A. Williams, "Experimental study on the effects of nose geometry on drag over axisymmetric bodies in supersonic flow", Department of Aerospace Engineering and Mechanics in the Graduate School of The University of Alabama.
- [4]. B. Kaleeswaran, S. Ranjith Kumar and Jeniwer Bimro. N, "An Aerodynamic Optimization of Supersonic Flow Over The Nose Section of Missiles", *International Journal of Engineering Research & Technology (IJERT)*, Vol. 2 Issue 4, pp. 253-262.
- [5]. Ryan J. Felkel, "Effect of Different Nose Profiles on Subsonic Pressure Coefficients", *American Institute of Aeronautics and Astronautics*, pp. 1-10.
- [6]. Girish Kumar and Dr. Pravin V Honguntikar, "CFD Analysis of Transonic Flow over the Nose Cone of Aerial Vehicle".
- [7]. Bruhn, 'Analysis and Design of Flight Vehicle Structures', 2nd edition, Jacobs Publishing, Inc.

P. KIRAN KUMAR. "Analysis of Nose Cone of Missile". *International Journal of Engineering Research and Applications (IJERA)*, vol.10 (07), 2020, pp 24-35.